Aalborg Universitet

AALBORG UNIVERSITY
DENMARK

# On the Sensitivity Analysis in Reliability Evaluation for Power Electronic Converters

Song, Yubo; Schirmer, Pascal A.; Schreivogel, Peter; Zhang, Kaichen; Wang, Huai; Blaabjerg, Frede

*Published in:*
IEEE Transactions on Power Electronics

*DOI (link to publication from Publisher):*
10.1109/TPEL.2025.3530148

*Creative Commons License*
CC BY 4.0

*Publication date:*
2025

*Document Version*
Accepted author manuscript, peer reviewed version

Link to publication from Aalborg University

*Citation for published version (APA):*
Song, Y., Schirmer, P. A., Schreivogel, P., Zhang, K., Wang, H., & Blaabjerg, F. (2025). On the Sensitivity Analysis in Reliability Evaluation for Power Electronic Converters. *IEEE Transactions on Power Electronics*, *40*(5), 7251 - 7260. Article 10842466. Advance online publication. https://doi.org/10.1109/TPEL.2025.3530148

**General rights**
Copyright and moral rights for the publications made accessible in the public portal are retained by the authors and/or other copyright owners and it is a condition of accessing publications that users recognise and abide by the legal requirements associated with these rights.

- Users may download and print one copy of any publication from the public portal for the purpose of private study or research.
- You may not further distribute the material or use it for any profit-making activity or commercial gain
- You may freely distribute the URL identifying the publication in the public portal -

**Take down policy**
If you believe that this document breaches copyright please contact us at vbn@aub.aau.dk providing details, and we will remove access to the work immediately and investigate your claim.

Downloaded from vbn.aau.dk on: April 23, 2025

# On the Sensitivity Analysis in Reliability Evaluation for Power Electronic Converters

Yubo Song, *Member, IEEE*, Pascal A. Schirmer, Peter Schreivogel,
Kaichen Zhang, *Member, IEEE*, Huai Wang, *Senior Member, IEEE*, and Frede Blaabjerg, *Fellow, IEEE*

***Abstract*—Power electronic converters are essential in modern electrical and electronic applications, necessitating the study on power electronic reliability for dependable design and operation. In earlier research on power electronic reliability, the mission profiles have been mapped to thermal stresses and lifetimes, while its applications are generally focused on steady-state scenarios. It turns out to be time-consuming and inefficient to repeat the entire procedures for addressing the impact of stress variances or model uncertainties. In this context, this article defines the sensitivity for power electronic reliability and provides a sensitivity-based perspective on system optimization, where the concept is formulated through two steps accounting for thermal stresses and lifetime respectively. The applications of sensitivities for thermal stresses and lifetime are demonstrated, which serve as identifiers of critical factors and quantitative metrics of marginal performances. Upon this, possibilities are also emerging for enhancing the cost-effectiveness of reliability validations and encompassing model robustness into reliability analysis and prediction.**

***Index Terms*—Power electronics, converters, reliability, sensitivity analysis, thermal stresses, lifetime.**

## I. Introduction

**P**OWER electronic converters have become the core interfaces of diverse electrical and electronic applications [1], [2], where power semiconductors play critical roles. With energy conversion being one of the primary functional requirements, the efficiency and power density of power electronic converters have been improved with cutting-edge components, topologies and operation strategies, etc. [3], [4], [5]. Meanwhile, acknowledged as a critical performance metric, reliability has emerged to be another key dimension of performances of power electronic applications during long-term field operation [6], which can be leveraged to reduce the overall economic costs including maintenance. In this context, the *lifetime* of components and systems, stemming from conventional reliability engineering, has become one of the critical metrics.

The large variation of power electronic components has made it challenging to develop empirical models comprehensively embracing all types of components. Going beyond the experience-driven methodologies described by failure rate [7], reliability analysis through component *failure mechanisms* (or physics-of-failure, PoF) is suggested [8], which navigates the lab tests and can handily adapt the reliability models to varied mission profiles.

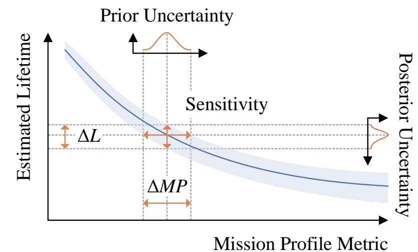


Fig. 1. Forming sensitivity analysis for power electronic reliability. Sensitivity serves as an effective metric mapping the prior uncertainty of mission profiles ($\Delta MP$) into posterior uncertainty of lifetime ($\Delta L$).

One of the typical types of failures of power electronic converters, wear-out failures, are dependent on the degradation of components [9]. Power semiconductors and capacitors are generally among the major components prone to wear-out failures [10], and the operational stresses influence how fast components will degrade. Thermal stresses, for instance, can typically be influenced by the converter topology and thermal interactions, but compromise among the components is often inevitable. To best distribute the stresses and achieve longer lifetime at the system level, it is thus worthwhile to optimize the design and operation of converters based on reliability models and / or metrics, namely the reliability-oriented design [11], [12], [13] and control [14], [15], [16].

Previous literature like [17] has enlightened a widely-used framework of mission profile based reliability analysis for power electronic converters. The lifetimes of components and the entire system are evaluated by analyzing the thermal stresses, which originate from mission profiles as per the PoF. However, when considering the influences of small-signal perturbations / uncertainties like errors or drifts of the parameters or mission profiles, it can be time-consuming to repeat the process of thermal evaluation, which normally concerns slow dynamics and long timescales. In addition, quantification of small-signal perturbations / uncertainties is also the key to enhance the robustness of reliability modeling, which has not yet been well explored either.

Inspired by the sensitivity analysis of power systems [18], this article thereby aims to unravel this aspect in power electronic reliability optimization, formulating *sensitivity* likewise for power electronic reliability that can serve as an instructive

This work is supported by BMW Group, Munich, Germany.

Yubo Song, Kaichen Zhang, Huai Wang and Frede Blaabjerg are with the Department of Energy (AAU Energy), Aalborg University, Aalborg, Denmark. (e-mail: {yuboso, kzh, hwa, fbl}@energy.aau.dk)

Pascal A. Schirmer and Peter Schreivogel are with BMW Group Research and Innovation Center, Munich, Germany. (e-mail: {Pascal.Schirmer, Peter.Schreivogel}@bmw.de)

(*Corresponding author: Yubo Song and Pascal Schirmer*)

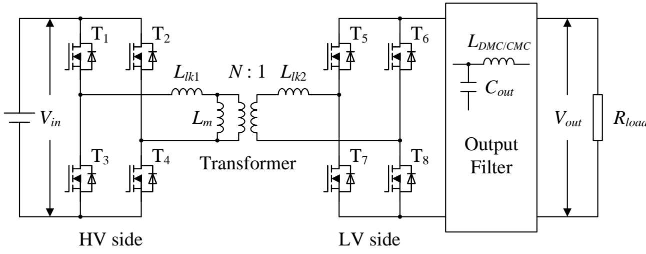


Fig. 2. The dual-active-bridge (DAB) converter studied in this article, which is divided into high-voltage (HV) side and low-voltage (LV) side.

TABLE I
RATED PARAMETERS OF THE STUDIED SYSTEM

| Parameters | Value |
|---|---|
| Input voltage $V_{\text{in}}$ | 200 V |
| Output voltage $V_{\text{out}}$ | 13.5 V |
| Switching frequency $f_{\text{sw}}$ | 100 kHz |
| Loading power $P_{\text{load}}$ | 1800 W |
| Trafo. transformation ratio $N$:1 | 10:1 |
| Trafo. leakage inductance $L_{\text{lk1,2}}$ | 1 µH, 0.02 µH |
| Output filter capacitance $C_{\text{out}}$ | 5.5 µF |
| Ambient temperature $T_{\text{amb}}$ | 35 °C |
| Power rating of HV devices | 750 V, 20 A |
| Power rating of LV devices | 100 V, 300 A |

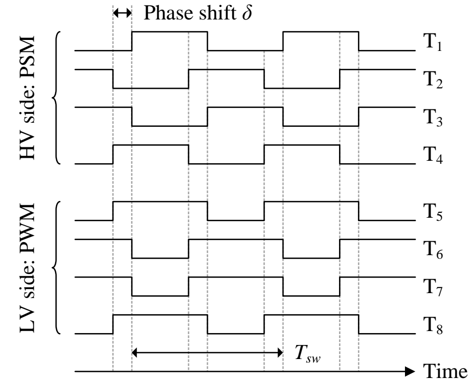


Fig. 3. Illustration of the drive signals for the modulation method adopted in this article for the studied DAB converter in Fig. 2.

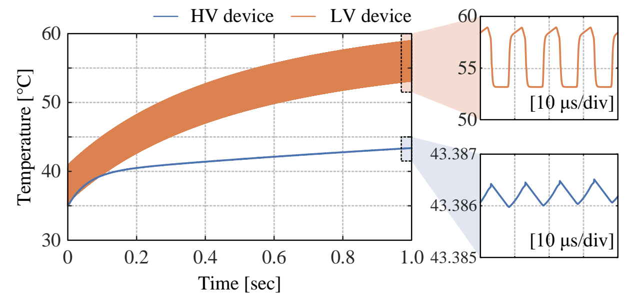


Fig. 4. Example of junction temperatures rising over time, where both the mean junction temperature and temperature swing have impacts on the lifetime of devices.

metric indicating the role of small-signal perturbations / uncertainties, as illustrated in Fig. 1. In general, prior variation or uncertainty of mission profiles ($\Delta MP$) introduces posterior variation or uncertainty of lifetime ($\Delta L$) as per the physics, and the changing rate formulates the said *sensitivity*, quantifying system performances under disturbances. Different from the probabilistic sensitivity for reliability engineering in [19], this article emphasizes the role of PoF in power electronic applications, and defines sensitivity in two steps as aligned with the reliability evaluation for power electronics, concerning the thermal stresses and estimated lifetime. By demonstrating their applications with case studies, the significance is highlighted in providing guidelines for operational sensing and optimizing the design of power electronic converters.

This article is organized as follows. Section II elaborates on the reliability model of power electronic components adopted. Sections III and IV introduce the concepts of sensitivity in reliability analysis for thermal stresses and lifetime, respectively, and how it can be leveraged in power electronic applications, through demonstrations on industrial case studies. Section V extends on discussions from the perspective of industrial testing and manufacturing. Section VI concludes the entire article with future visions on this topic.

## II. Thermal Stresses and Reliability Modeling of Power Electronic Converters

The reliability of power electronic converters is normally evaluated based on the physics-of-failure (PoF) of power electronic components [8] highlighting the roles of mission profiles and thermal stresses, which is employed in this article. To manifest this, a dual-active-bridge (DAB) DC-DC converter is selected as the study case, of which the topology is illustrated in Fig. 2, and key parameters of the case illustrated in Fig. 2 are specified in Table I unless otherwise specified. The HV and LV sides operate in phase-shift modulation (PSM) and pulse-width modulation (PWM), respectively, and exemplary drive signals are accordingly depicted in Fig. 3.

The power semiconductors (SiC MOSFETs from Infineon with preliminary datasheets) in the study case are preliminarily identified as the most critical and fragile components. Without loss of generality, other components like capacitors are assumed to be sufficiently reliable throughout the analysis, considering that they operate under approximately constant mission profiles, and they are relatively less sensitive to the studied mission profiles.

The widely-used lifetime models of power semiconductors (both IGBT [20] and SiC [21]) are deduced from power cycling tests. The models combine the Coffin-Manson Law and the Arrhenius Law [22], which can be expressed as (1). The cycles of junction temperature (power cycles, as shown in Fig. 4) lead to the mechanical stresses which accumulate over time, and the lifetime, in number of cycles, is principally influenced by the junction temperature $T_{\text{j}}$ (mean value $T_{\text{j,m}}$ or minimum value $T_{\text{j,min}}$ over the power cycles) and the magnitude of its swing $\Delta T_{\text{j}}$ in the power cycles, as well as other key factors including ON-state time (or temperature-rising time) $t_{\text{on}}$, bondwire current $I_{\text{bw}}$, voltage level $V$ and

bondwire diameter $D$, as in:

$$N_f = N_0 \cdot \Delta T_{\mathrm{j}}^{\beta_1} \cdot \exp\left(\frac{\beta_2}{T_{\mathrm{j}}}\right) \cdot t_{\mathrm{on}}^{\beta_3} \cdot I_{\mathrm{bw}}^{\beta_4} \cdot V^{\beta_5} \cdot D^{\beta_6} \quad (1)$$

where, $T_{\mathrm{j}}$ is in Kelvin (K), $N_f$ is the estimated lifetime in number of cycles, and $N_0$, $\beta_1$, $\beta_2$, $\beta_3$, $\beta_4$, $\beta_5$ and $\beta_6$ are the coefficients obtained from experimental tests.

***Remark 1*: It should be noted that the model specified by (1) only involves the most primary failure mechanisms for power semiconductors, and all the factors are assumed not to deviate significantly from the rated conditions. Encompassing more factors may impel additional terms in the product, and irregular factors may need to be described by specialized lifetime models.**

In this article, it is assumed that the change of ON-state time $t_{\mathrm{on}}$ has negligible influence, and the bondwire current $I_{\mathrm{bw}}$, voltage level $V$ and bondwire diameter $D$ do not change by cases. Thus, the corresponding terms can be absorbed into $N_0$ as a more inclusive coefficient $N_0'$, namely:

$$N_f = N_0' \cdot \Delta T_{\mathrm{j}}^{\beta_1} \cdot \exp\left(\frac{\beta_2}{T_{\mathrm{j}}}\right) \quad (2)$$

The power cycles can thereby be classified based on the mission profiles $\{T_{\mathrm{j}}, \Delta T_{\mathrm{j}}\}$.

***Remark 2***: The power cycles are identical and evenly distributed over time in the case depicted in Fig. 4, the number of which is therefore proportional to time periods. In more general cases, the power cycles aroused by time-variant loading profiles should be analyzed in groups via *rain-flow counting*.

***Remark 3***: It should be noted here that the lifetime in the model formulated by (1) and (2) stands for the $B_x$ lifetime (an estimation of the worn-out testing samples reaches $x\%$ of the entire population), where $x$ is specified by the application of interest and reflected in the coefficients extracted from the testing results. In this article, it is assumed that the device samples also follow the model coefficients in [20] and [21], yielding $B_{10}$ lifetime.

To efficiently calculate $\{T_{\mathrm{j}}, \Delta T_{\mathrm{j}}\}$ for a semiconductor stack-up as illustrated in Fig. 5(a), Model Order Reduction (MOR) techniques can be used [23]. In the present study thermal relations are modeled based on electrical series network representations also called Foster models [24]. In details, both the thermal path from the junction of a semiconductor, as well as the thermal path from the semiconductor case to the ambient are modeled.

In Fig. 5(b) a Foster network with $K$ layers is shown, including a thermal resistance ($R_{\mathrm{th}}^k$) and a thermal capacitance ($C_{\mathrm{th}}^k$) for each layer, a loss source ($P_{\mathrm{loss}}$) and a reference temperature ($T_{\mathrm{amb}}$), e.g. the ambient or coolant temperature. The transient thermal impedance can then be modeled as in (3) using a set of $K$ exponential functions.

$$Z_{\mathrm{th}} = \sum_{k=1}^{K} R_{\mathrm{th}}^k \left(1 - e^{-t/\tau_k}\right) \quad (3)$$

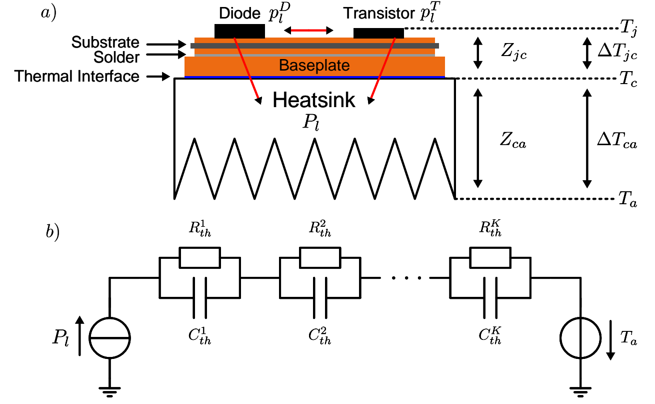


Fig. 5. Thermal semiconductor stack-up including chips, substrate, solder and baseplate (a), as well as reduced order thermal network using Foster network representation (b).

where $Z_{\mathrm{th}}(t)$ is the total transient thermal impedance and $\tau_k = R_{\mathrm{th}}^k C_{\mathrm{th}}^k$ is the time constant of the $k$-th layer. Consequently $T_{\mathrm{j}}$ can be calculated as:

$$T_{\mathrm{j}} = T_{\mathrm{amb}} + \Delta T_{\mathrm{j}} = T_{\mathrm{amb}} + P_{\mathrm{loss}} * (Z_{\mathrm{ca}} + Z_{\mathrm{jc}}) \quad (4)$$

where "*" denotes the convolution of the transient thermal impedance $Z_{\mathrm{ca/jc}}$ with the power losses $P_{\mathrm{loss}}$. It should be noted that it is assumed that $Z_{\mathrm{th}} = Z_{\mathrm{ca}} + Z_{\mathrm{jc}}$ already includes the coupling of transistor ($p_{\mathrm{loss}}^{\mathrm{T}}$) and diode losses ($p_{\mathrm{loss}}^{\mathrm{D}}$).

Based on the thermal stress caused by $\{T_{\mathrm{j}}, \Delta T_{\mathrm{j}}\}$, the lifetime can be translated into number of cycles to failure using (1) or (2) and subsequently into the time-to-failure by Miner's rule [25]. As expressed in (5), the operational damage or lifetime consumption of a power semiconductor, if normalized, accumulates by the number of endured power cycles from the beginning:

$$D = \sum_i \frac{n^{(i)}}{N_f^{(i)}} \quad (5)$$

where, $n^{(i)}$ and $N_f^{(i)}$ denote the counted number of the power cycles and corresponding cycles-to-failure, respectively, in the $i$-th time period, given that the studied time period is sufficiently short compared with the entire lifetime and the damage accumulation can be linearly approximated [25]. If multiple types of power cycles are involved, the normalized accumulated damage of a specific type of power cycles would be calculated as the number of the cycles $n^{(i,j)}$ divided by the corresponding cycles-to-failure $N_f^{(i,j)}$, which indicates the consumed proportion of total availability, and then, a sum is taken for all the individual damages as a linear combination indicating the overall damage accumulation.

By the end-of-life (EOL) of the device, the normalized damage $D$ should be approximately accumulated to 1 (or $100\%$ of the usable lifetime despite the types of mission profiles), thus $D$ can be mapped into the $B_x$ lifetime by considering the time length of the power cycles.

Moreover, the reliability of power devices can also be described as a probability of reliable operation, which is needed for system-level reliability evaluation for power elec-

tronic converters. The time-to-failure data generally follows the Weibull distribution as:

$$R(t) = \exp\left[-\left(\frac{t}{\eta}\right)^{\beta}\right] \tag{6}$$

where $\beta$ and $\eta$ are the shaping factor and the characteristic lifetime of the distribution, respectively. The aforementioned $B_x$ lifetime corresponds to the time instant $t$ when the accumulated probability of failure $F(t)$ equals $x\%$, or the reliability $R(t)$ equals $1 - x\%$.

If no redundant components are considered, then the system-level reliability of a power electronic converter requires all components to be reliable, which is:

$$R_{\text{sys}}(t) = \prod_{j} R_{\text{device}}^{(j)}(t) \tag{7}$$

By solving the equation $R_{\text{sys}}(t) = 1 - x\%$, the $B_x$ lifetime of the converter can be obtained, as the expected lifetime.

## III. Sensitivity Analysis on Thermal Stresses

The reliability of power electronic converters and systems is influenced by various factors in relation to mission profiles and system configurations, while the factors normally participate to distinct extents. To this end, the sensitivity in power electronic reliability analysis for typical scenarios is worthwhile to be defined. Generally, reliability analysis for power electronic converters and systems can be divided into two steps, the mapping from mission profiles to the stresses and from stresses to the lifetime. As it is not straightforward to map the mission profile metrics directly to lifetime, the sensitivity analysis will likewise be formulated based on the two steps and connected thereafter, which will be discussed in the following sections individually alongside demonstrations on industrial case studies.

### A. Formulating Sensitivity for Thermal Stresses

To facilitate the analysis, an exemplary scenario of the study case is first presented in Fig. 6. The thermal stresses, or more specifically, junction temperature $T_{\text{j}}$ and its swing $\Delta T_{\text{j}}$ as per Section II, are influenced by the loading power $P_{\text{load}}$ and the ambient temperature $T_{\text{amb}}$, while the rate of change may vary for different stress metrics or different devices.

It is reasonable to assume the relationships from mission profiles to thermal stresses to be continuous and differentiable. To describe this, the sensitivity matrix of thermal stresses can be defined as:

$$\mathbf{J}_{\text{T}} = \begin{bmatrix} \dfrac{\partial T_{\text{j}}}{\partial P_{\text{load}}} & \dfrac{\partial T_{\text{j}}}{\partial T_{\text{amb}}} \\ \dfrac{\partial \Delta T_{\text{j}}}{\partial P_{\text{load}}} & \dfrac{\partial \Delta T_{\text{j}}}{\partial T_{\text{amb}}} \end{bmatrix} \tag{8}$$

Or more generally, the sensitivity analysis can be extended to other system configuration or mission profile metrics, as:

$$\mathbf{J}_{\text{T}}(\boldsymbol{\xi}) = \nabla_{\boldsymbol{\xi}} \mathbf{T} \tag{9}$$

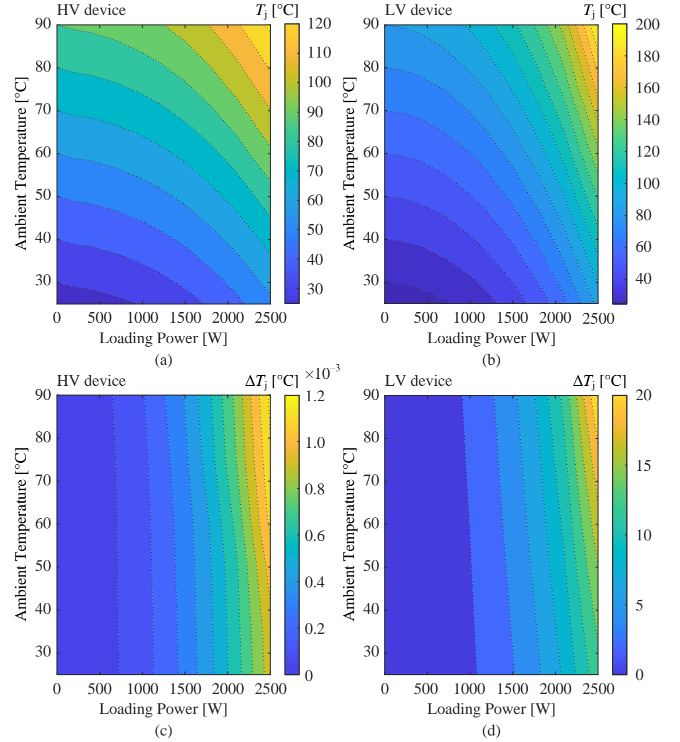


Fig. 6. Contour plot of the thermal stress metrics $T_{\text{j}}$ and $\Delta T_{\text{j}}$ subject to the mission profile metrics $T_{\text{amb}}$ and $P_{\text{load}}$ for HV and LV switches: (a) and (b) mean junction temperatures $T_{\text{j}}$, and (c) and (d) junction temperature swings $\Delta T_{\text{j}}$ in the power cycles.

where, $\mathbf{T}$ stands for the vector for thermal stresses and $\boldsymbol{\xi}$ for studied mission profile metrics. It is numerically equivalent to the Jacobian matrix between the stresses and mission profiles.

An example is given based on (8), where the sensitivity matrix of the study case is calculated and depicted in Fig. 7. The sensitivities of HV and LV devices do not exhibit identical trends as a result of different loss models, and the monotonicity can be dependent on whether conduction or switching loss plays a more dominant role. In general, the following points can be inferred:

1) The precision required for sensing and control for testing or operation under condition monitoring. For example, if a $\pm 10\%$ variation of the loading power $P_{\text{load}}$ is studied around the rated value 1800 W, then the junction temperature $T_{\text{j}}$ of HV device will change by around 3.1 °C, which should be able to be detected and distinguished by the employed thermal sensors.
2) If the stresses are sensitive to mission profiles, then in case of, e.g., active thermal control of power electronic converters, higher robustness should be underlined concerning mission profile uncertainty.

Furthermore, the analytical expressions of the mapping relationships from mission profiles to the thermal stresses can be complicated and inconsistent for different scenarios. Consequently, a convenient approach is to quantify the relationships into numerical fittings (e.g., polynomial expressions) based on the data from simulations or tests at a number of operation

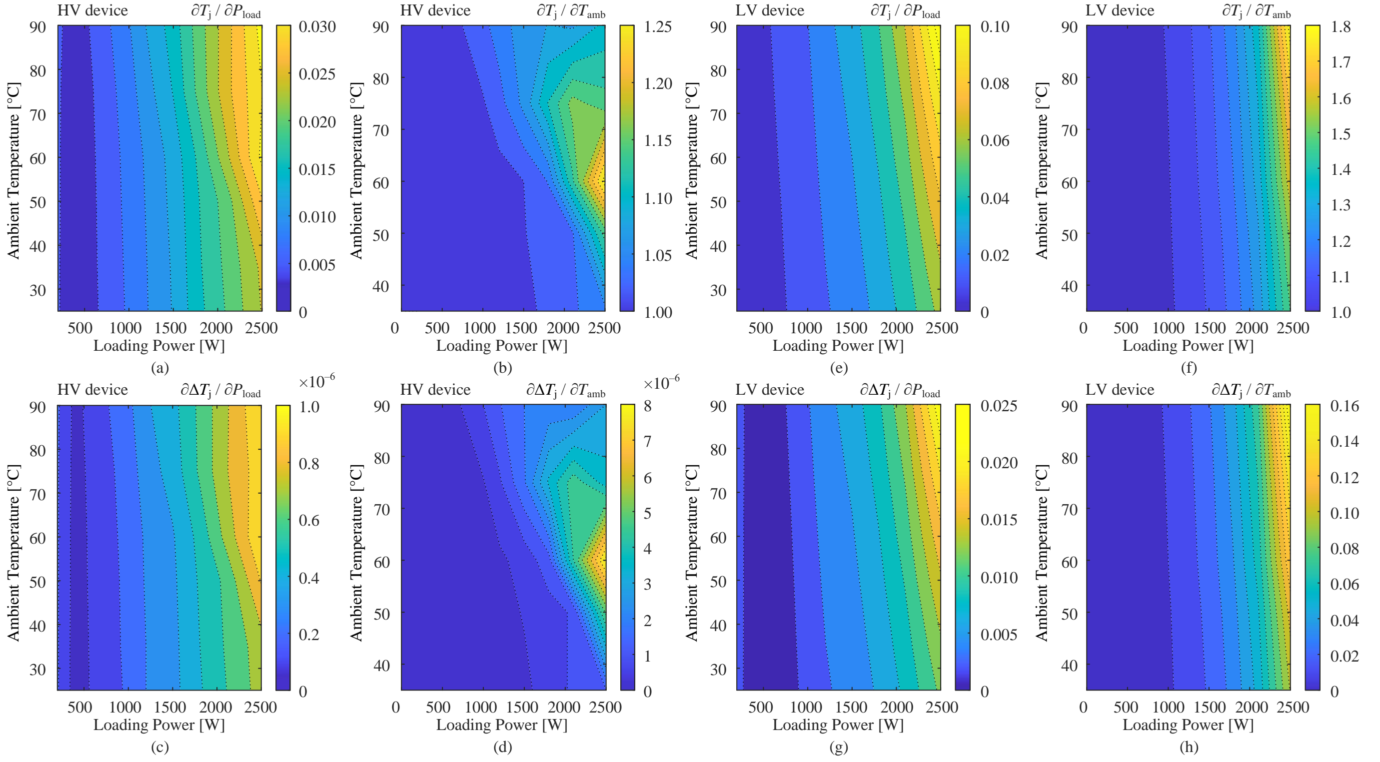


Fig. 7. Thermal stress sensitivity of the studied devices subject to the mission profile metrics $T_{\mathrm{amb}}$ and $P_{\mathrm{load}}$: (a)-(d) for HV device, and (e)-(h) for LV device. The sensitivity metrics are labeled to the top of each sub-figure individually.

points, like:

$$\begin{aligned}\hat{T}_{\mathrm{j}} &= f_1\left(P_{\mathrm{load}}, T_{\mathrm{amb}}\right)\\ \hat{T}_{\mathrm{jsw}} &= f_2\left(P_{\mathrm{load}}, T_{\mathrm{amb}}\right)\end{aligned} \tag{10}$$

where $f_1(\cdot)$ and $f_2(\cdot)$ are derived polynomial fitting functions. Then the sensitivity matrix can alternatively be expressed into:

$$\mathbf{J}_{\mathrm{T}} \approx \begin{bmatrix} \dfrac{\partial f_1}{\partial P_{\mathrm{load}}} & \dfrac{\partial f_1}{\partial T_{\mathrm{amb}}} \\ \dfrac{\partial f_2}{\partial P_{\mathrm{load}}} & \dfrac{\partial f_2}{\partial T_{\mathrm{amb}}} \end{bmatrix} \tag{11}$$

The thermal stresses can then be estimated based on the following equation as per the Taylor's Theorem:

$$\Delta\begin{bmatrix} T_{\mathrm{j}} \\ \Delta T_{\mathrm{j}} \end{bmatrix} = \mathbf{J}_{\mathrm{T}}\Delta\begin{bmatrix} P_{\mathrm{load}} \\ T_{\mathrm{amb}} \end{bmatrix} + o\left(\left\|\Delta\begin{bmatrix} P_{\mathrm{load}} \\ T_{\mathrm{amb}} \end{bmatrix}\right\|\right) \tag{12}$$

where $o(\cdot)$ denotes higher-order infinitesimal terms. In a more general form, (12) can be expressed as:

$$\Delta\mathbf{T} = \mathbf{J}_{\mathrm{T}}(\boldsymbol{\xi})\Delta\boldsymbol{\xi} + o\left(\|\Delta\boldsymbol{\xi}\|\right) \approx \mathbf{J}_{\mathrm{T}}\Delta\boldsymbol{\xi} \tag{13}$$

The small-signal influences of mission profile uncertainties can thus be quantified.

From this perspective, sensitivity analysis can be employed to account for mission profile uncertainties in reliability modeling, thereby laying the basis for robust reliability-oriented control for power electronic converters and systems.

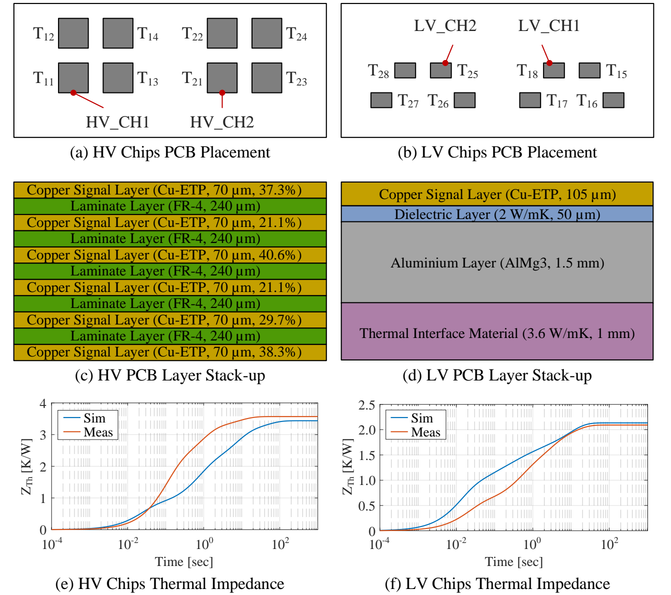


Fig. 8. Illustration of the layout of the DAB system under test, including the chip placement in (a) and (b), the layer stack-up of the PCBs in (c) and (d), and the measured (*Meas.* in the legends of (d) and (f)) as well as simulated (*Sim.* in the legends of (d) and (f)) transient thermal impedance curves for HV (left) and LV boards (right) respectively.

## *B. Extensions with Experimental Testing Results*

To further manifest the applications of sensitivity analysis, an industrial DAB converter system from BMW is thereby

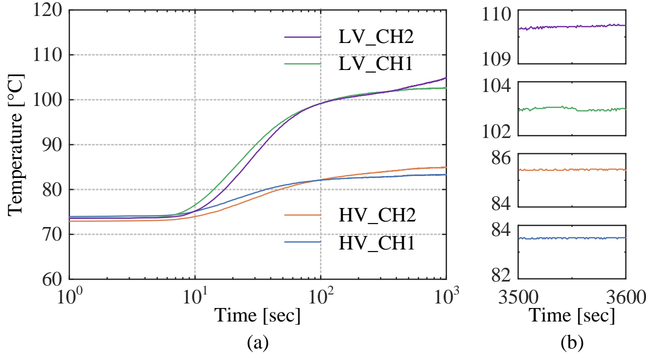


Fig. 9. Exemplary temperature rise data measured by thermocouples during the test where $T_{\mathrm{amb}}$ = 75 °C, including: (a) heating-up process, and (b) steady-state temperature.

TABLE II
DEVICE TEMPERATURE MEASUREMENTS AND SENSITIVITY ANALYSIS WITH EXPERIMENTAL TESTS

| Measured Devices | Coolant Temperature | | | | | $\frac{\partial T_{\mathrm{c}}}{\partial T_{\mathrm{amb}}}$ |
|---|---|---|---|---|---|---|
| | 35 °C | 45 °C | 55 °C | 65 °C | 75 °C | |
| HV_CH1 | 46.3 | 55.9 | 65.3 | 74.3 | 83.5 | 0.93 |
| HV_CH2 | 50.0 | 59.0 | 67.9 | 76.4 | 85.4 | 0.88 |
| LV_CH1 | 71.8 | 80.2 | 88.1 | 95.2 | 103.0 | 0.77 |
| LV_CH2 | 78.1 | 87.0 | 99.6 | 103.9 | 110.7 | 0.82 |

Note: All temperature data in °C.

studied and tested by validating the stress differences among the devices in the same system during regular operations. The layout of the study case is illustrated in Fig. 8. In details, Fig. 8 includes the chip placement in the $x$-$y$ plane, the layer stack-up in $z$-direction, and the measured as well as calculated transient thermal impedance curves. Two channels are placed in each circuit board, and the system is divided into HV and LV boards. Temperatures are measured by thermocouples touching the surface of power devices, which however should be the case temperatures $T_{\mathrm{c}}$ but are generally in positive correlation with the junction temperatures or thermal stresses. The measurements are identified as labeled in Fig. 8.

A group of the measurement results is presented in Fig. 9. The temperatures rise over time, meanwhile the differences are shown among the components, due to the inconsistencies in component parameters and spacial positioning in practice. Following this point, experimental tests are conducted where the coolant temperature is varied, with the results shown in Table II.

It is noticed that in this case the measured case temperatures approximately increase linearly upon the coolant temperature. Hence, the sensitivity $\partial T_{\mathrm{c}}/\partial T_{\mathrm{amb}}$ is calculated as the slope of the linear fitting of the relationship, which is also shown in Table II. This sensitivity is physically determined by the thermal networks between the devices and the ambient, and helps to identify the sources of stresses on the devices. For example, by comparing HV devices, CH1 ($T_{11}$) is 5.7% more sensitive to the change of ambient temperature due to the spacial design in relation to the heat dissipation as well as thermal coupling with other components, while CH2 ($T_{21}$) ends up with suffering from higher stress, which should be recognized as a consequence of self-heating.

## IV. SENSITIVITY ANALYSIS ON LIFETIME

### A. Sensitivity from the Lifetime Model

Similar to Section III, the sensitivity for the lifetime can be formulated, which is more transparent with the lifetime model in Section II from the thermal stresses. By taking the partial derivatives of $N_f$ in (1) or (2), the sensitivity for the lifetime (in number of cycles) can be defined as following:

$$S_{N_f}(\Delta T_{\mathrm{j}}) = \frac{\partial N_f}{\partial \Delta T_{\mathrm{j}}} = N_f \cdot \left(\beta_1 \Delta T_{\mathrm{j}}^{-1}\right) \tag{14a}$$

$$S_{N_f}(T_{\mathrm{j}}) = \frac{\partial N_f}{\partial T_{\mathrm{j}}} = N_f \cdot \left(-\beta_2 T_{\mathrm{j}}^{-2}\right) \tag{14b}$$

In this way, the change of device lifetime is quantified upon small-signal variances of stresses, which is determined by the type of device. By extracting $N_f$ from (14), the sensitivity can be expressed into the normalized form as:

$$S_{N_f}^{(\mathrm{n})}(\Delta T_{\mathrm{j}}) = \frac{\partial N_f / N_f}{\partial \Delta T_{\mathrm{j}} / \Delta T_{\mathrm{j}}} = \beta_1 \tag{15a}$$

$$S_{N_f}^{(\mathrm{n})}(T_{\mathrm{j}}) = \frac{\partial N_f / N_f}{\partial T_{\mathrm{j}}} = -\beta_2 T_{\mathrm{j}}^{-2} \tag{15b}$$

where, (15a) and (15b) are the normalized sensitivity subject to per-unit change of $\Delta T_{\mathrm{j}}$ and per-degree change of $T_{\mathrm{j}}$, respectively. In the context of (15), the exact value of $N_f$ is not a must in the sensitivity analysis.

***Remark 4***: The sensitivity (14) and (15) in this section are formulated for power semiconductors based on their lifetime models. For other components like capacitors (e.g., [26]), the formula may not be in an identical form which stems from the Coffin-Manson Law or Arrhenius Law, whereas the basic idea and the framework should hold for different lifetime models.

The sensitivity analysis on $T_{\mathrm{j}}$ and $\Delta T_{\mathrm{j}}$ can then be decoupled from each other after normalization. Besides, the two equations can be interpreted as the following, through an exemplary case where the coefficients are specified as $\beta_1$ = –3.775 and $\beta_2$ = 1285, [20], [21], without loss of generality:

1) From (15a), every 1% larger temperature swing $\Delta T_{\mathrm{j}}$ induces $|\beta_1|$% shorter estimated lifetime, where $\beta_1 < 0$ (3.78% decrease in the example).
2) With (15b), the normalized lifetime sensitivity of the study case can be deduced as plotted in Fig. 10. For example, around the operation point of $T_{\mathrm{j}}$ = 60 °C, every 1 °C decrease of junction temperature $T_{\mathrm{j}}$ corresponds to an estimation of 1.15% longer lifetime.

### B. Evaluations on the Total Sensitivity

Subsequently, the sensitivity from mission profiles to the lifetime is formulated by connecting the two steps. Considering the entire procedures of reliability evaluation, the sensitivity of lifetime in relation to mission profiles can be

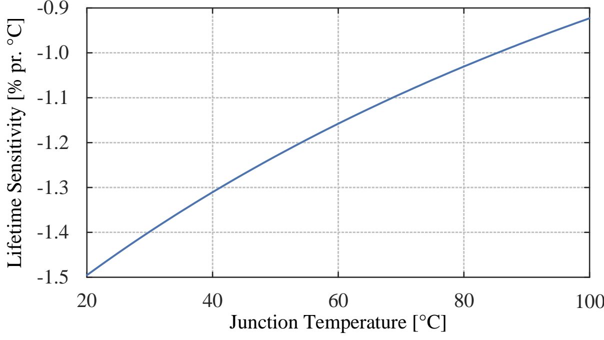


Fig. 10. Normalized sensitivity of lifetime subject to junction temperature.

defined according to the chain rule, which is exemplified as following if assuming only $T_\mathrm{j}$ and $\Delta T_\mathrm{j}$ are influenced by the mission profile metrics $P_\mathrm{load}$ and $T_\mathrm{amb}$:

$$S_{N_f}(P_\mathrm{load}) = \frac{\partial N_f}{\partial P_\mathrm{load}} = \frac{\partial N_f}{\partial T_\mathrm{j}} \cdot \frac{\partial T_\mathrm{j}}{\partial P_\mathrm{load}} + \frac{\partial N_f}{\partial \Delta T_\mathrm{j}} \cdot \frac{\partial \Delta T_\mathrm{j}}{\partial P_\mathrm{load}} \quad (16a)$$

$$S_{N_f}(T_\mathrm{amb}) = \frac{\partial N_f}{\partial T_\mathrm{amb}} = \frac{\partial N_f}{\partial T_\mathrm{j}} \cdot \frac{\partial T_\mathrm{j}}{\partial T_\mathrm{amb}} + \frac{\partial N_f}{\partial \Delta T_\mathrm{j}} \cdot \frac{\partial \Delta T_\mathrm{j}}{\partial T_\mathrm{amb}} \quad (16b)$$

In more general cases, if one denotes all studied mission profile metrics and relevant stress metrics as $\xi_i$ and $\sigma_j$, respectively, then (16) can be summarized into:

$$S_{N_f}(\xi_i) = \frac{\partial N_f}{\partial \xi_i} = \sum_j \frac{\partial N_f}{\partial \sigma_j} \cdot \frac{\partial \sigma_j}{\partial \xi_i} \quad (17)$$

where $\partial N_f / \partial \sigma_j$ and $\partial \sigma_j / \partial \xi_i$ correspond to the aforementioned definitions (14) and (8), respectively. Similar to (15), (17) can also be normalized as:

$$S^{(\mathrm{n})}_{N_f}(\xi_i) = \frac{\partial N_f / N_f}{\partial \xi_i / \xi_i} = \sum_j \frac{\partial N_f}{\partial \sigma_j} \cdot \frac{\partial \sigma_j}{\partial \xi_i} \cdot \left( \frac{N_f}{\xi_i} \right)^{-1} \quad (18)$$

which denotes the percentage variation of $N_f$ with regard to per-unit change of $\xi_i$.

Or alternatively, (17) can be written in the form of total differential for addressing the absolute variation of lifetime $\mathrm{d}N_f$ accounting for the change of all mission profile metrics:

$$\mathrm{d}N_f = \sum_i \sum_j \frac{\partial N_f}{\partial \sigma_j} \cdot \frac{\partial \sigma_j}{\partial \xi_i} \cdot \mathrm{d}\xi_i \quad (19)$$

Based on this, the lifetime sensitivity in relation to the mission profiles is calculated as shown in Fig. 11, in percentage of $N_f$. The lifetime sensitivity reflects the overall influence of both mission profiles and the type of devices, including a balance of the different gradients in terms of $\Delta T_\mathrm{j}$ and $T_\mathrm{j}$ according to (14a) and (14b), eventually inducing a non-monotonic trend of variation. In contrast to Fig. 7, the results can be interpreted as:

1) The sensitivity is mapped to the sensing precision in the other way. If, e.g., a 1% error of lifetime estimation is acceptable when $\partial N_f / \partial T_\mathrm{amb}$ = –1.0%/°C, then an approximation of 1 °C sensing precision is sufficient.
2) When the lifetime is sensitive to the variation of mission profiles, there will be a larger variance of the estimated lifetime, which should also be noted, e.g., in reliability-oriented design and control, to ensure the robustness of the system models.
3) In terms of robustness, the error of measurement is a typical consideration. For example, it can be derived from (14) that the deviation of the sensitivity would be relevant to the relative rate of error in terms of the absolute measurement.

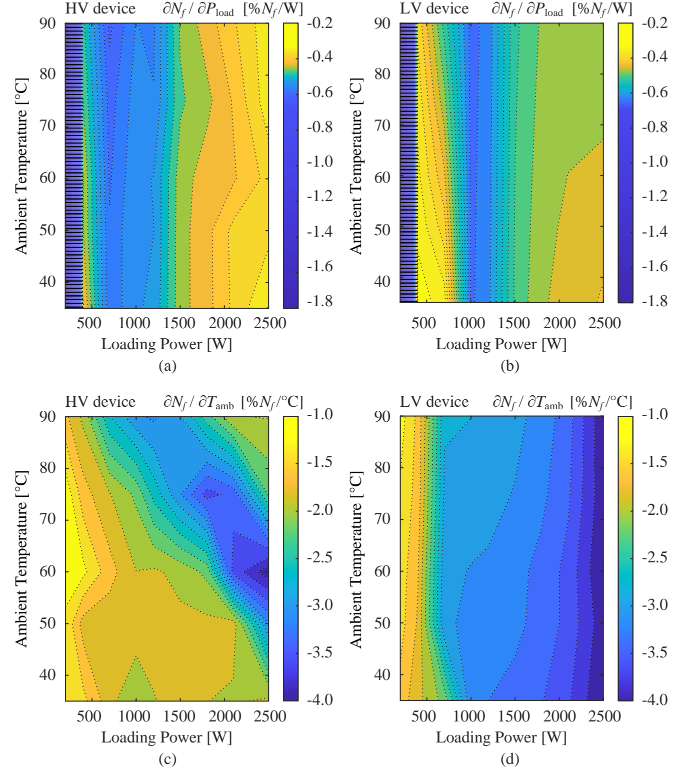


Fig. 11. Lifetime sensitivity of the studied devices in relation to the mission profile metrics $T_\mathrm{amb}$ and $P_\mathrm{load}$: (a), (c) for HV device, and (b), (d) for LV device. The sensitivity metrics are labeled to the top of each sub-figure individually.

After all, more comprehensive validations of the sensitivity analysis require long-term tests under more varied mission profiles, which is not elaborated in this article due to the availability of lab facilities. In practice, it should also be noted that the sensitivity analysis for lifetime should act as comparative guidelines of reliability-oriented design approaches for power electronic systems, rather than fixed and explicit performance codes.

## V. Extended Discussions

It is worth noting, that the thermal impedance presented in Section II also features an uncertainty, which can result from manufacturing tolerances, measurement uncertainties or modeling assumptions. We hereby extend the validations to lifetime sensitivity analysis on circuit parameter variations (equivalent transformer leakage inductance $L_\mathrm{lk1}$ and output filter capacitance $C_\mathrm{out}$), with simulated results presented in Table III. The average sensitivity is preliminarily exemplified, while a more accurate approach can be plotting the sensitivity alongside different parameter values. In any case, different

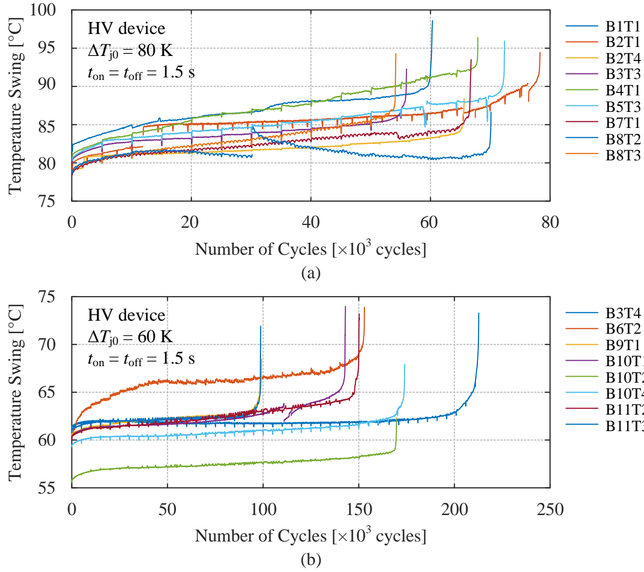


Fig. 12. Experimental results of power cycling tests of the studied power semiconductor devices for HV-side converter, under initial conditions: (a) $\Delta T_\mathrm{j}$ = 80 K, and (b) $\Delta T_\mathrm{j}$ = 60 K, $t_\mathrm{on}$ = $t_\mathrm{off}$ = 1.5 s. The tests are conducted on several converter boards configured identically as specified in Fig. 8, HV boards, and $\mathrm{B}_x\mathrm{T}_y$ denotes the group of test on the Converter Board $x$, Transistor $y$. The differences in junction temperature swings are demonstrated as time goes on, as a result of different $R_\mathrm{dson}$ increases related to device positions and manufacturing consistency.

coupling of circuit components with the power devices are implied, which is a practical concern and worth being encompassed into more robust design of power electronic systems.

The scatter due to manufacturing tolerances is of particular importance for industrial applications, where the reliability must be ensured for a large number of manufactured devices. Fig. 12 preliminarily exhibits an example of the error in consistency due to manufacturing of the devices. The differences of devices lead to varied lifetime obtained from power cycling tests, which should be described by statistical distributions. In principle, the most significant thermal impedance variations result from layers within the thermal path that have a high thermal resistance, e.g. thermal interfaces or electrical insulation with a low thermal conductivity. The thermal resistance of these layers is most sensitive to the thermal conductivity and to tolerances of the gap width or layer thickness, while additional variations may originate from voids inside the thermal interface material. Depending on the thermal coupling within the electronic component, losses of adjacent components may also influence the fit of a thermal impedance model. Typical sources for power loss variations can be electrical contact resistances or the drain-source resistance of transistors.

Similarly, the positions of devices on the PCBs may also lead to differences in thermal paths, including both the thermal paths to the ambient and the inter-device thermal coupling. It can also be seen from Fig. 12 the differences of devices within the same board and even the same arm of the converter. In hardware design, it is preferred to conduct thermal routing and align the power losses prior to implementation, to ensure prolonged overall system lifetime, where sensitivity analysis can be employed as an assistive tool.

To address this aspect, Monte Carlo simulations on the thermal performance, where probability distributions of geometrical tolerances and material properties are used, are one of the means to predict the overall uncertainty of a thermal resistance. In most cases geometrical tolerances can be approximated with a Gaussian distribution while material properties or losses are bounded and require one-sided distributions e.g. log-normal. There are multiple ways to obtain the probability distributions during the initial design phase. In case of electronic components, distributions or at least upper and lower bounds might be supplied by the manufacturers. The tolerances of geometrical dimensions are typically defined based on experience and later on ensured by process capability analysis during the industrialization. Additional effects like contact resistances or scattering in thermal conductivity of thermal interface materials can be considered assuming upper and lower bounds. With this, the sensitivity of reliability can be handily evaluated, as an effective reference for enhancing the liability of industrial manufacturing and reducing the unforeseen costs.

TABLE III
NORMALIZED LIFETIME OF THE STUDY CASE AND SENSITIVITY ACCOUNTING FOR PARAMETER UNCERTAINTIES

| $L_\mathrm{lk1}$ | 0.5 μH | 1.0 μH | 1.5 μH | Average Sensitivity |
|---|---|---|---|---|
| HV | 1.059 | 1.000 | 0.961 | –0.098 [$\%N_\mathrm{f}/\ \%L_\mathrm{lk1}$] |
| LV | 1.004 | 1.000 | 1.000 | –0.004 [$\%N_\mathrm{f}/\ \%L_\mathrm{lk1}$] |
| $C_\mathrm{out}$ | 2.75 μF | 5.50 μF | 8.25 μF | Average Sensitivity |
| HV | 0.984 | 1.000 | 0.992 | 0.008 [$\%N_\mathrm{f}/\ \%C_\mathrm{out}$] |
| LV | 0.989 | 1.000 | 1.003 | 0.014 [$\%N_\mathrm{f}/\ \%C_\mathrm{out}$] |

Note: Estimated lifetime is normalized based on the rated condition.

## VI. CONCLUSIONS

This article has elaborated on the sensitivity analysis in reliability analysis for power electronic converters in order to address the need of small-signal analysis and provide proper interpretations therein. In this article, the sensitivity analysis is mathematically defined and explicated through two steps, highlighting the thermal stresses and lifetime models, respectively, and the influences of mission profiles are eventually portrayed. Case studies have also been rendered, which include both simulation and experimental testing results.

It can be concluded that sensitivity can not only guide the design and thermal monitoring of power electronic converters and systems, but also act as effective metrics for encompassing robustness into reliability modeling and prediction. Therefore, potential future extension of this topic can be applications of this metric into practice, accounting for robustness in reliability modeling and control as well as stimulating effectiveness-optimized design of power electronic converters and systems.

## REFERENCES


[1] D. Boroyevich, I. Cvetković, D. Dong, R. Burgos, F. Wang, and F. Lee, "Future Electronic Power Distribution Systems a Contemplative View," in *Proc. 2010 12th International Conference on Optimization of Electrical and Electronic Equipment*, 2010, pp. 1369–1380.

[2] J. Carrasco, L. Franquelo, J. Bialasiewicz, E. Galvan, R. PortilloGuisado, M. Prats, J. Leon, and N. Moreno-Alfonso, "Power-Electronic Systems for the Grid Integration of Renewable Energy Sources: A Survey," *IEEE Trans. Ind. Electron.*, vol. 53, no. 4, pp. 1002–1016, 2006.

[3] J. Biela, M. Schweizer, S. Waffler, and J. W. Kolar, "SiC versus Si—Evaluation of Potentials for Performance Improvement of Inverter and DC–DC Converter Systems by SiC Power Semiconductors," *IEEE Trans. Ind. Electron.*, vol. 58, no. 7, pp. 2872–2882, 2011.

[4] K. A. Kim, Y.-C. Liu, M.-C. Chen, and H.-J. Chiu, "Opening the Box: Survey of High Power Density Inverter Techniques from the Little Box Challenge," *CPSS Trans. Power Electron. Appl.*, vol. 2, no. 2, pp. 131–139, 2017.

[5] M. Hossain, N. Rahim, and J. a/l Selvaraj, "Recent Progress and Development on Power DC-DC Converter Topology, Control, Design and Applications: A Review," *Renewable Sustainable Energy Rev.*, vol. 81, pp. 205–230, 2018.

[6] H. Wang and F. Blaabjerg, "Power Electronics Reliability: State of the Art and Outlook," *IEEE J. Emerging Sel. Top. Power Electron.*, vol. 9, no. 6, pp. 6476–6493, 2021.

[7] Y. Song and B. Wang, "Survey on Reliability of Power Electronic Systems," *IEEE Trans. Power Electron.*, vol. 28, no. 1, pp. 591–604, 2013.

[8] H. Wang, M. Liserre, F. Blaabjerg, P. de Place Rimmen, J. B. Jacobsen, T. Kvisgaard, and J. Landkildehus, "Transitioning to Physics-of-Failure as a Reliability Driver in Power Electronics," *IEEE J. Emerging Sel. Top. Power Electron.*, vol. 2, no. 1, pp. 97–114, 2014.

[9] S. Rahimpour, H. Tarzamni, N. V. Kurdkandi, O. Husev, D. Vinnikov, and F. Tahami, "An Overview of Lifetime Management of Power Electronic Converters," *IEEE Access*, vol. 10, pp. 109 688–109 711, 2022.

[10] S. Yang, A. Bryant, P. Mawby, D. Xiang, L. Ran, and P. Tavner, "An Industry-Based Survey of Reliability in Power Electronic Converters," *IEEE Trans. Ind. Appl.*, vol. 47, no. 3, pp. 1441–1451, 2011.

[11] H. Wang, K. Ma, and F. Blaabjerg, "Design for Reliability of Power Electronic Systems," in *Proc. IECON 2012 - 38th Annual Conference on IEEE Industrial Electronics Society*, 2012, pp. 33–44.

[12] T. Dragičević, P. Wheeler, and F. Blaabjerg, "Artificial Intelligence Aided Automated Design for Reliability of Power Electronic Systems," *IEEE Trans. Power Electron.*, vol. 34, no. 8, pp. 7161–7171, 2019.

[13] J. V. M. Farias, A. F. Cupertino, V. d. N. Ferreira, H. A. Pereira, S. I. Seleme, and R. Teodorescu, "Reliability-Oriented Design of Modular Multilevel Converters for Medium-Voltage STATCOM," *IEEE Trans. Ind. Electron.*, vol. 67, no. 8, pp. 6206–6214, 2020.

[14] J. Kuprat, C. H. van der Broeck, M. Andresen, S. Kalker, M. Liserre, and R. W. De Doncker, "Research on Active Thermal Control: Actual Status and Future Trends," *IEEE J. Emerging Sel. Top. Power Electron.*, vol. 9, no. 6, pp. 6494–6506, 2021.

[15] M. Andresen, M. Liserre, and G. Buticchi, "Review of Active Thermal and Lifetime Control Techniques for Power Electronic Modules," in *Proc. 2014 16th European Conference on Power Electronics and Applications*, 2014, pp. 1–10.

[16] J. Falck, M. Andresen, and M. Liserre, "Active Thermal Control of IGBT Power Electronic Converters," in *Proc. IECON 2015 - 41st Annual Conference of the IEEE Industrial Electronics Society*, 2015, pp. 1–6.

[17] D. Zhou, H. Wang, and F. Blaabjerg, "Mission Profile Based System-Level Reliability Analysis of DC/DC Converters for a Backup Power Application," *IEEE Trans. Power Electron.*, vol. 33, no. 9, pp. 8030–8039, 2018.

[18] P. Kundur, *Power System Stability and Control*, 1st ed. McGraw-Hill, 1994.

[19] J. He and X. Guan, "Uncertainty Sensitivity Analysis for Reliability Problems with Parametric Distributions," *IEEE Trans. Reliab.*, vol. 66, no. 3, pp. 712–721, 2017.

[20] R. Bayerer, T. Herrmann, T. Licht, J. Lutz, and M. Feller, "Model for Power Cycling Lifetime of IGBT Modules - Various Factors Influencing Lifetime," in *Proc. 5th International Conference on Integrated Power Electronics Systems*, 2008, pp. 1–6.

[21] F. Hoffmann, N. Kaminski, and S. Schmitt, "Comparison of the Power Cycling Performance of Silicon and Silicon Carbide Power Devices in a Baseplate Less Module Package at Different Temperature Swings," in *Proc. 2021 33rd International Symposium on Power Semiconductor Devices and ICs (ISPSD)*, 2021, pp. 175–178.

[22] A. Birolini, *Reliability Engineering*, 8th ed. Springer, 2017.

[23] X. Dong, A. Griffo, and J. Wang, "Multiparameter Model Order Reduction for Thermal Modeling of Power Electronics," *IEEE Trans. Power Electron.*, vol. 35, no. 8, pp. 8550–8558, 2020.

[24] M. N. Touzelbaev, J. Miler, Y. Yang, G. Refai-Ahmed, and K. E. Goodson, "High-Efficiency Transient Temperature Calculations for Applications in Dynamic Thermal Management of Electronic Devices," *J. Electron. Packag.*, vol. 135, no. 3, pp. 031 001, 1–7, 2013.

[25] M. A. Miner, "Cumulative Damage in Fatigue," *J. Appl. Mech.*, vol. 12, no. 3, pp. A159–A164, 1945.

[26] H. Wang and F. Blaabjerg, "Reliability of Capacitors for DC-Link Applications in Power Electronic Converters—An Overview," *IEEE Trans. Ind. Appl.*, vol. 50, no. 5, pp. 3569–3578, 2014.


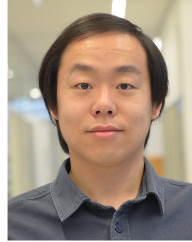


**Yubo Song** (Member, IEEE) received the B.Sc. and M.Eng. degrees in Electrical Engineering from Shanghai Jiao Tong University, Shanghai, China, in 2016 and 2019, and Ph.D. degree in Energy Technology from Aalborg University, Aalborg, Denmark, in 2023, respectively. He is currently a Postdoc in the Department of Energy, Aalborg University, Aalborg, Denmark.

From May to July 2022, he was a visiting researcher with the ELITE Grid Research Lab, University of Alberta, Edmonton, AB, Canada. He is a recipient of the Spin-Outs Denmark grant in 2024.

His research interests include the control, stability and reliability of power electronic systems and power electronic dominated grids.

**Pascal A. Schirmer** received the B.Eng. degree in electrical engineering from the University of Applied Sciences, Esslingen, Germany, in 2018, and the Ph.D. degree in electrical engineering from the University of Hertfordshire, UK, in 2021. Since 2021, he has been working in the R&D department at BMW AG, Munich, Germany, where he is responsible for the lifetime evaluation of power electronic systems. Furthermore, he is a visiting research fellow at the University of Hertfordshire, UK, where he focuses on NILM (software and hardware applications), and a visiting lecturer on electro-mobility at the TAE, Esslingen, Germany.

**Peter Schreivogel** received the Dipl.-Ing. degree in aerospace engineering from the Technical University Dresden in 2009, a Research Master from the Von Karman Institute for Fluid Dynamics, Rhode-Saint-Genèse, Belgium, in 2011 and the Ph.D. in aerospace engineering from the University of the Federal Armed Forces Munich in 2015.

From 2015 to 2018, he worked as a thermo-fluid systems engineer at Rolls-Royce Deutschland. Since 2018, he has been a specialist in thermal management of power electronics with the BMW AG, Munich. His research interests include advanced cooling technologies like pulsating heat pipes and reduced order thermal modeling. Dr. Schreivogel was a recipient of the DLR technology award in 2009 and the Claudius Dornier jr. dissertation award in 2016.


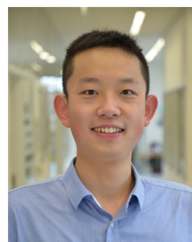


**Kaichen Zhang** (Member, IEEE) received the B.Eng. degree in electrical engineering and automation from Huazhong University of Science and Technology, Wuhan, China, in 2018, and the M.S. degree in energy technology (power electronics and drives) in 2020 from Aalborg University, Aalborg, Denmark, where he is currently pursuing the Ph.D. degree.

From September 2019 to February 2020, he was with ABB Corporate Research Center, Baden-Dättwil, Switzerland. His research interests include the reliability of power electronic components.

**Huai Wang** (Senior Member, IEEE) received the B.E. degree in electrical engineering from Huazhong University of Science and Technology, Wuhan, China, in 2007 and a Ph.D. degree in power electronics from the City University of Hong Kong in 2012. He is currently a Professor with AAU Energy at Aalborg University, Denmark, where he leads the group of Reliability of Power Electronic Converters (ReliaPEC) and the mission on Digital Transformation and AI. He was a Visiting Scientist with the ETH Zurich, Switzerland, from Aug. to Sep. 2014, and with the Massachusetts Institute of Technology (MIT), USA, from Sep. to Nov. 2013. He was with the ABB Corporate Research Center, Switzerland, in 2009. His research addresses the fundamental challenges in modeling and validating power electronic component failure mechanisms and application issues in system-level predictability, condition monitoring, circuit architecture, and robustness design.

Dr. Wang received the Richard M. Bass Outstanding Young Power Electronics Engineer Award from the IEEE Power Electronics Society in 2016 and the 1st Prize Paper Award from IEEE Transactions on Power Electronics in 2021. He serves as an Associate Editor of JOURNAL OF EMERGING AND SELECTED TOPICS IN POWER ELECTRONICS and IEEE TRANSACTIONS ON POWER ELECTRONICS. He was elected as a member of the Danish Academy of Technical Sciences in 2023.

**Frede Blaabjerg** (Fellow, IEEE) received the Ph.D. degree in electrical engineering from Aalborg University, Aalborg, Denmark, in 1995.

He was with ABB-Scandia, Randers, Denmark, from 1987 to 1988. He became an Assistant Professor in 1992, an Associate Professor in 1996, and a Full Professor of power electronics and drives in 1998. From 2017 he became a Villum Investigator. He is *honoris causa* at University Politehnica Timisoara (UPT), Romania, and Tallinn Technical University (TTU) in Estonia. His current research interests include power electronics and its applications, such as in wind turbines, PV systems, reliability, harmonics, and adjustable speed drives. He has published more than 600 journal papers in the fields of power electronics and its applications. He is the co-author of four monographs and editor of ten books in power electronics and its applications.

He has received 32 IEEE Prize Paper Awards, the IEEE PELS Distinguished Service Award in 2009, the EPE-PEMC Council Award in 2010, the IEEE William E. Newell Power Electronics Award 2014, the Villum Kann Rasmussen Research Award 2014, the Global Energy uPrize in 2019 and the 2020 IEEE Edison Medal. He was the Editor-in-Chief of the IEEE TRANSACTIONS ON POWER ELECTRONICS from 2006 to 2012. He has been a Distinguished Lecturer for the IEEE Power Electronics Society from 2005 to 2007 and for the IEEE Industry Applications Society from 2010 to 2011 as well as 2017 to 2018. In 2019-2020 he served as President of the IEEE Power Electronics Society. He is Vice-President of the Danish Academy of Technical Sciences too. He is nominated in 2014-2019 by Thomson Reuters to be between the most 250 cited researchers in Engineering in the world.